

The $X(3872)$ and the search for its bottomonium counterpart at the LHC

K. Toms^{*†}

University of New Mexico, USA

E-mail: ktoms@cern.ch

We present results on $X(3872)$ particle studies at three LHC experiments: ATLAS, CMS, and LHCb. Production cross section measurements are reported, as well as determination of the $X(3872)$ quantum numbers. The search of the $X(3872)$ bottomonium counterpart is also described.

*38th International Conference on High Energy Physics
3-10 August 2016
Chicago, USA*

^{*}Speaker.

[†]On behalf of the ATLAS, CMS, and LHCb collaborations.

1. Introduction

The $X(3872)$ particle was first discovered by the Belle experiment in 2003 in the transition $B^\pm \rightarrow K^\pm X (\rightarrow J/\psi \pi^+ \pi^-)$ [1] and soon was confirmed by many experiments [2]. The $X(3872)$ state is narrow, with mass close to the $D^0 \bar{D}^{*0}$ threshold and decays to the $\rho^0 J/\psi$ and $\omega J/\psi$ final states with comparable branching fractions, thus violating isospin symmetry, so it cannot be a simple $c\bar{c}$ state. The nature of the state remains unclear, and there are many theoretical developments that suggest different models to describe the $X(3872)$ structure, see for example [3]. Heavy quark symmetry implies the existence of a hidden-beauty partner, X_b , which should be produced in pp collisions.

In this paper we present the results by three LHC [4] experiments: ATLAS [5], CMS [6], and LHCb [7], related to the studies of $X(3872)$ properties and search for its bottomonium counterpart.

2. Search for X_b at ATLAS and CMS

The decay $X_b \rightarrow \pi^+ \pi^- \Upsilon(1S) (\rightarrow \mu^+ \mu^-)$ may serve as a decay mode analogous to that in which the $X(3872)$ was discovered. CMS reported results on a search for this decay, finding no evidence for narrow states in the 10.06-10.31 GeV and 10.40-10.99 GeV mass ranges [8]. Upper limits on the product of cross section and branching fraction at values between 0.9% and 5.4% of the $\Upsilon(2S)$ rate were set. The resulting plot is shown in Figure 1 right. ATLAS has performed a similar search [9] with results shown in Figure 1 left, and no evidence for new narrow states with masses in the range 10.05-10.31 GeV and 10.40-11.00 GeV was found. Separate fits to the $\Upsilon(1^3D_J)$ triplet, $\Upsilon(10860)$, and $\Upsilon(11020)$ also reveal no significant signals.

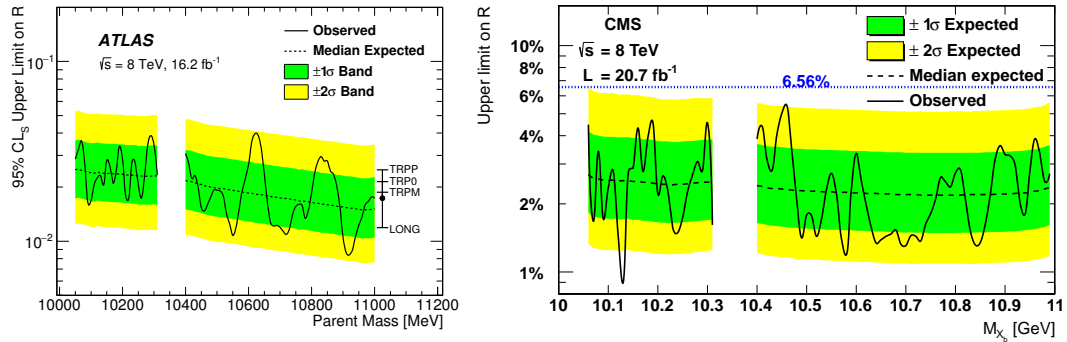


Figure 1: **Left:** Observed 95% CL_S upper limits (solid line) on the relative production rate $R = (\sigma B)/(\sigma B)_{2S}$ of a hypothetical X_b parent state decaying isotropically to $\pi^+ \pi^- \Upsilon(1S)$, as a function of mass. The median expectation (dashed) and the corresponding $\pm 1\sigma$ and $\pm 2\sigma$ bands (green and yellow respectively) are also shown. The bar on the right shows typical shifts under alternative X_b spin-alignment scenarios, relative to the isotropic (“FLAT”) case shown with the solid points [9]. **Right:** Upper limits at the 95% confidence level on R , the production cross section for the X_b times its branching fraction to $\Upsilon(1S)\pi^+\pi^-$ relative to the $\Upsilon(2S)$, as a function of the X_b mass. The solid curve shows the observed limits, while the dashed curve represents the expected limits in the absence of a signal, with the two shaded regions giving the ± 1 and ± 2 standard deviation uncertainties on the expected limits. The measured value for the analogous $X(3872)$ to $\psi(2S)$ ratio of 6.56% is shown by the dotted line [8].

3. Production measurement of $\psi(2S)$ and $X(3872)$ at ATLAS and CMS

A cross-section measurement of promptly produced $X(3872)$ was performed by CMS [10] at $\sqrt{s} = 7$ TeV as a function of transverse momentum p_T . It was done in a kinematic range in which the $X(3872)$ had $(10 < p_T < 50)$ GeV and rapidity $|y| < 1.2$. The ratio of the $X(3872)$ and $\psi(2S)$ cross sections times their branching fractions into $J/\psi \pi^+ \pi^-$ was measured as a function of p_T . It has been shown that the nonrelativistic QCD (NRQCD) prediction [11] for prompt $X(3872)$ production, assuming a $D^0 \bar{D}^{*0}$ molecule, is too high, although the shape of the p_T dependence was described fairly well. A later interpretation of

the $X(3872)$ as a mixed $\chi_{c1}(2P) - D^0\bar{D}^{*0}$ state, where the $X(3872)$ is produced predominantly through its $\chi_{c1}(2P)$ component, was adopted in conjunction with the next-to-leading-order (NLO) NRQCD model and fitted to CMS data, showing a good agreement [12]. ATLAS has performed a similar study at $\sqrt{s}=8$ TeV [13] with the $J/\psi\pi^+\pi^-$ candidates having ($10 < p_T < 70$) GeV and $|y| < 0.75$. Two models of the lifetime dependence of the non-prompt production are considered: a model with a single effective lifetime, and an alternative model with two distinctly different effective lifetimes. The two models give compatible results for the prompt and non-prompt differential cross sections of the $\psi(2S)$ and $X(3872)$. For the single-lifetime model, assuming that non-prompt $\psi(2S)$ and $X(3872)$ originate from the same mix of parent b -hadrons, the following result is obtained for the ratio of the branching fractions:

$$R_B^{1L} = \frac{\mathcal{B}(B \rightarrow X(3872) + \text{any})\mathcal{B}(X(3872) \rightarrow J/\psi\pi^+\pi^-)}{\mathcal{B}(B \rightarrow \psi(2S) + \text{any})\mathcal{B}(\psi(2S) \rightarrow J/\psi\pi^+\pi^-)} = (3.95 \pm 0.32(\text{stat}) \pm 0.08(\text{sys})) \times 10^{-2},$$

[13]. In the two-lifetime model, the two lifetimes are fixed to expected values for $X(3872)$ originating from the decays of the B_c and from long-lived b -hadrons, respectively, with their relative weight determined from the fits to the data. The ratio of the branching fractions R_B is determined from the long-lived component alone:

$$R_B^{2L} = \frac{\mathcal{B}(B \rightarrow X(3872) + \text{any})\mathcal{B}(X(3872) \rightarrow J/\psi\pi^+\pi^-)}{\mathcal{B}(B \rightarrow \psi(2S) + \text{any})\mathcal{B}(\psi(2S) \rightarrow J/\psi\pi^+\pi^-)} = (3.57 \pm 0.33(\text{stat}) \pm 0.11(\text{sys})) \times 10^{-2},$$

[13]. In the two-lifetime model, the fraction of the short-lived non-prompt component in $X(3872)$ production, for $p_T > 10$ GeV, is found to be

$$\frac{\sigma(pp \rightarrow B_c + \text{any})\mathcal{B}(B_c \rightarrow X(3872) + \text{any})}{\sigma(pp \rightarrow \text{non-prompt } X(3872) + \text{any})} = (25 \pm 13(\text{stat}) \pm 2(\text{sys}) \pm 5(\text{spin}))\%, \quad (3.1)$$

[13]. The measured differential cross section for non-prompt production of the $X(3872)$ is shown in Figure 2 (right). This is compared to a calculation based on the FONLL model prediction for $\psi(2S)$, recalculated for the $X(3872)$ using a kinematic template [13] for the non-prompt $X(3872)/\psi(2S)$ ratio and the effective value of the product of the branching fractions $\mathcal{B}(B \rightarrow X(3872))\mathcal{B}(X(3872) \rightarrow J/\psi\pi^+\pi^-) = (1.9 \pm 0.8) \times 10^{-4}$ estimated in Ref. 3.1 based on Tevatron data [15]. This calculation overestimates the data by a factor increasing with p_T from about four to about eight over the p_T range of this measurement. The non-prompt fractions of $\psi(2S)$ and $X(3872)$ production are shown in Figure 3. The non-prompt fraction of $X(3872)$ shows no sizeable dependence on p_T . This measurement agrees within uncertainties with the CMS result obtained at $\sqrt{s}=7$ TeV [10].

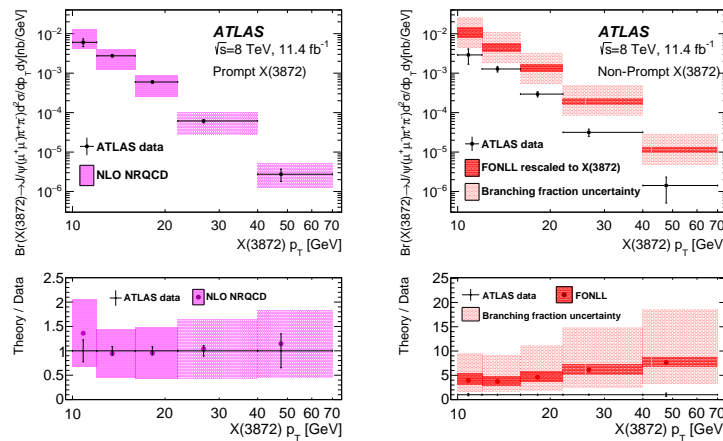


Figure 2: Measured cross section times branching fractions as a function of p_T for (left) prompt $X(3872)$ in the ATLAS experiment [13] compared to NLO NRQCD predictions with the $X(3872)$ modelled as a mixture of $\chi_{c1}(2P)$ and a $D^0\bar{D}^{*0}$ molecular state [12], and (right) non-prompt $X(3872)$ compared to the FONLL [14] model prediction. Bottom plots on both left and right show theory to data ratio.

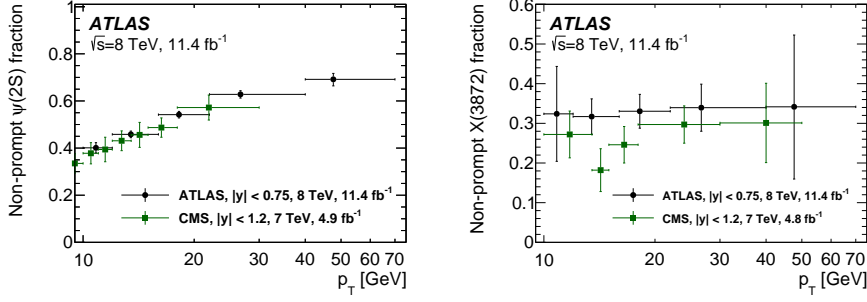


Figure 3: Measured non-prompt fractions for (left) $\psi(2S)$ and (right) $X(3872)$ production in the ATLAS experiment [13], compared to CMS results [10] at $\sqrt{s} = 7$ TeV. The blue circles are the results reported by ATLAS, while the green squares show CMS results [10, 16].

4. Determination of the $X(3872)$ quantum numbers at LHCb

Early constraints on the $X(3872)$ quantum numbers were set by CDF [17] and have restricted the options to 1^{++} and 2^{-+} . LHCb's 2013 full angular analysis [18] settled on 1^{++} , but that analysis assumed that the lowest orbital angular momentum process dominated the decay. A new analysis [19] described below removed that assumption. The analysis uses 3 fb^{-1} of $\sqrt{s} = 7$ TeV and $\sqrt{s} = 8$ TeV data.

The $X(3872)$ signal is sought in the decay $B^+ \rightarrow X(3872)K^+$ with $X(3872) \rightarrow \rho^0 J/\psi$, $\rho^0 \rightarrow \pi^+ \pi^-$, and $J/\psi \rightarrow \mu^+ \mu^-$. The fit yields 1011 ± 38 signal events over a background of 1468 ± 44 in the ΔM range of (725–825) MeV. The $X(3872)$ mass resolution is 2.8 MeV. The signal purity is 80% within 2.5 standard deviations around the peak.

Angular correlations in the B^+ decay chain are analyzed using an unbinned maximum-likelihood fit to determine the $X(3872)$ quantum numbers and orbital angular momentum. The probability density function (\mathcal{P}) for each J^{PC} hypothesis, J_X , is defined in the five-dimensional angular space $\Omega \equiv (\cos\theta_X, \cos\theta_\rho, \Delta\phi_{X,\rho}, \cos\theta_{J/\psi}, \Delta\phi_{X,J/\psi})$, where θ_X , θ_ρ and $\theta_{J/\psi}$ are the helicity angles in the $X(3872)$, ρ^0 and J/ψ decays, respectively, and $\Delta\phi_{X,\rho}$ and $\Delta\phi_{X,J/\psi}$ are the angles between the decay planes of the $X(3872)$ particle and its decay products. The quantity \mathcal{P} is the normalized product of the expected decay matrix element (\mathcal{M}) squared and the reconstruction efficiency (ε), $\mathcal{P}(\Omega|J_X) = |\mathcal{M}(\Omega|J_X)|^2 \varepsilon(\Omega) / I(J_X)$, where $I(J_X) = \int |\mathcal{M}(\Omega|J_X)|^2 \varepsilon(\Omega) d\Omega$. The efficiency is averaged over the $\pi^+ \pi^-$ mass of the $X(3872) \rightarrow \rho^0 J/\psi$, $\rho^0 \rightarrow \pi^+ \pi^-$ decay. The lineshape of the ρ^0 resonance can change slightly depending on the $X(3872)$ spin hypothesis. The effect on $\varepsilon(\Omega)$ is very small and is neglected. The angular correlations are obtained using the helicity formalism,

$$|\mathcal{M}(\Omega|J_X)|^2 = \sum_{\Delta\lambda_\mu = -1, +1} \left| \sum_{\lambda_{J/\psi}, \lambda_\rho = -1, 0, +1} A_{\lambda_{J/\psi}, \lambda_\rho} D_{0, \lambda_{J/\psi} - \lambda_\rho}^{J_X} (0, \theta_X, 0)^* D_{\lambda_\rho, 0}^1(\Delta\phi_{X,\rho}, \theta_\rho, 0)^* D_{\lambda_{J/\psi}, \Delta\lambda_\mu}^1(\Delta\phi_{X,J/\psi}, \theta_{J/\psi}, 0)^* \right|^2,$$

where the λ 's are particle helicities, $\Delta\lambda_\mu = \lambda_{\mu^+} - \lambda_{\mu^-}$, and the $D_{\lambda_1, \lambda_2}^J$ are Wigner functions. The helicity couplings, $A_{\lambda_{J/\psi}, \lambda_\rho}$, are expressed in terms of the LS couplings, B_{LS} , through Clebsch-Gordan coefficients, where L is the orbital angular momentum between the ρ^0 and the J/ψ mesons, and S is the sum of their spins. The possible values of L are constrained by parity conservation, $P_X = P_{J/\psi} P_\rho (-1)^L = (-1)^L$. In this analysis all L values are allowed. Values of J_X up to four are analyzed. Since the orbital angular momentum in the B^+ decay equals J_X , high values are suppressed by the angular momentum barrier. The set of possible complex B_{LS} amplitudes, which are free parameters in the fit, is denoted as α . The function to be minimized is $-2 \ln \mathcal{L}(J_X, \alpha) \equiv -s_w 2 \sum_{i=1}^{N_{\text{data}}} w_i \ln \mathcal{P}(\Omega_i | J_X, \alpha)$, where $\mathcal{L}(J_X, \alpha)$ is the unbinned likelihood and N_{data} is the number of selected candidates. The background is subtracted using the *sPlot* technique [20]

by assigning a weight, w_i , to each candidate based on its ΔM value. No correlations between ΔM and Ω are observed. Prompt production of $X(3872)$ in pp collisions gives negligible contribution to the selected sample. Statistical fluctuations in the background subtraction are taken into account in the log-likelihood value via a constant scaling factor, $s_w = \sum_{i=1}^{N_{\text{data}}} w_i / \sum_{i=1}^{N_{\text{data}}} w_i^2$. The 1^{++} hypothesis gives the highest likelihood value. Projections of the data and of the fit \mathcal{P} onto individual angles show good consistency with the 1^{++} assignment as is illustrated in Fig. 4 left. Inconsistency with the other assignments is apparent when correlations between various angles are examined. For example, the data projection onto $\cos\theta_X$ is consistent only with the 1^{++} fit projection after requiring $|\cos\theta_\rho| > 0.6$ (see Fig. 4 right), while inconsistency with the other quantum number assignments is less clear without the $\cos\theta_\rho$ requirement.

In summary, the analysis confirms that the eigenvalues of total angular momentum, parity, and charge-conjugation of the $X(3872)$ state are 1^{++} . These quantum numbers are consistent with those predicted by the molecular or tetraquark models and with the $\chi_{c1}(2^3P_1)$ charmonium state [21], possibly mixed with a molecule [22]. Other charmonium states are excluded. No significant D-wave fraction is found, with an upper limit of 4% at 95% C.L. The S-wave dominance is expected in the charmonium or tetraquark models, in which the $X(3872)$ state has a compact size. An extended size, as that predicted by the molecular model, implies more favorable conditions for the D wave. However, conclusive discrimination among models is difficult because quantitative predictions are not available.

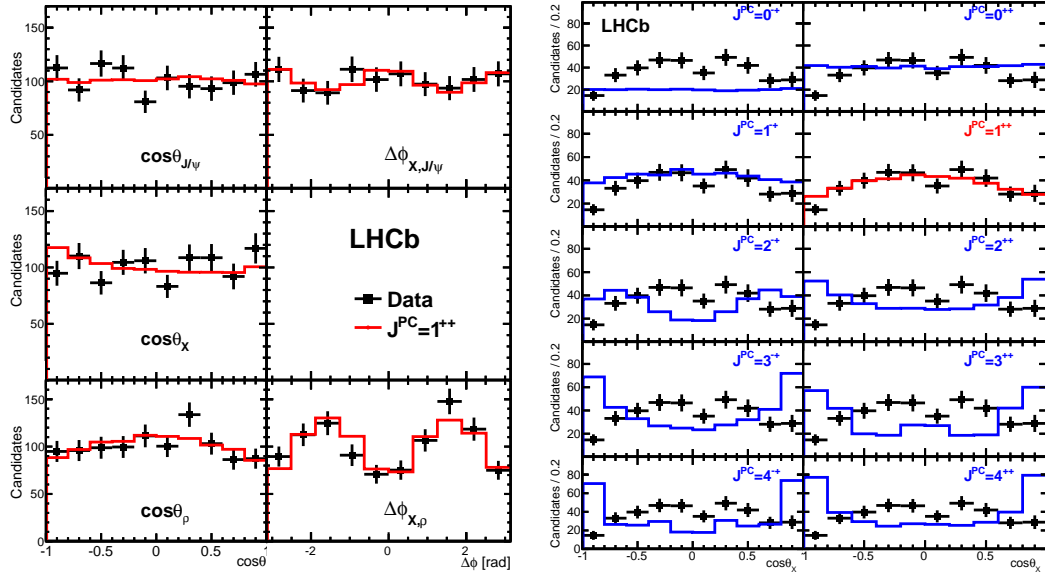


Figure 4: Left: Background-subtracted distributions of all angles for the data (points with error bars) and for the 1^{++} fit projections (solid histograms). Right: Background-subtracted distribution of $\cos\theta_X$ for candidates with $|\cos\theta_\rho| > 0.6$ for the data (points with error bars) compared to the expected distributions for various $X(3872)$ J^{PC} assignments (solid histograms) with the B_{LS} amplitudes obtained by the fit to the data in the five-dimensional angular space. The fit displays are normalized to the observed number of signal events in the full angular phase space.

References

- [1] S.-K. Choi, et al. (Belle Collaboration), Phys. Rev. Lett. 91 (2003) 262001, arXiv:hep-ex/0309032v2.
- [2] B. Aubert, et al. (BaBar Collaboration), Phys. Rev. D 71 (2005) 071103, arXiv:hep-ex/0406022.
D. Acosta, et al. (CDF Collaboration), Phys. Rev. Lett. 93 (2004) 072001, arXiv:hep-ex/0312021.
V. Abazov, et al. (D0 Collaboration), Phys. Rev. Lett. 93 (2004) 162002, arXiv:hep-ex/0405004.
- [3] E. S. Swanson, Phys. Lett. B 588 (2004) 189-195, arXiv:hep-ph/0311229.
L. Maiani, F. Piccinini, A. Polosa, V. Riquer, Phys. Rev. D 71 (2005) 014028, arXiv:hep-ph/0412098.
D. Ebert, R. Faustov, V. Galkin, Phys. Lett. B 634 (2006) 214-219, arXiv:hep-ph/0512230.

- [4] L. Evans and P. Bryant (editors) JINST 3 (2008) S08001.
- [5] ATLAS Collaboration, JINST 3 (2008) S08003.
- [6] CMS Collaboration, JINST 3 (2008) S08004.
- [7] LHCb collaboration, A. A. Alves Jr. et al., JINST 3 (2008) S08005.
LHCb collaboration, R. Aaij et al., Int. J. Mod. Phys. A30 (2015) 1530022, arXiv:1412.6352.
- [8] CMS Collaboration, Phys. Lett. B 727 (2013) 57-76, arXiv:1309.0250.
- [9] ATLAS Collaboration, Phys. Lett. B740 (2015) 199-217, arXiv:1410.4409.
- [10] CMS Collaboration, JHEP 04 (2013) 154, arXiv:1302.3968.
- [11] P. Artoisenet and E. Braaten, Phys. Rev. D 81 (2010) 114018, arXiv:0911.2016.
- [12] C. Meng, H. Han and K.-T. Chao, (2013), arXiv:1304.6710.
- [13] ATLAS Collaboration, arXiv:1610.09303, submitted to JHEP.
- [14] M. Cacciari et al., JHEP 10 (2012) 137, arXiv:1205.6344.
- [15] G. Bauer, Int. J. Mod. Phys. A 20 (2005) 3765-3767, arXiv:hep-ex/0409052.
- [16] CMS Collaboration, JHEP 02 (2012) 011, arXiv:1111.1557.
- [17] A. Abulencia et al., (CDF Collaboration), Phys. Rev. Lett. 96 (2006) 102002, arXiv:hep-ex/0512074.
- [18] R. Aaij et al. (LHCb Collaboration), Phys. Rev. Lett. 110 (2013) 222001, arXiv:1302.6269.
- [19] R. Aaij et al. (LHCb Collaboration), Phys. Rev. D 92 (2015) 011102, arXiv:1504.06339.
- [20] M. Pivk and F. R. Le Diberder, Nucl. Instrum. Meth. A555 (2005) 356, arXiv:physics/0402083.
- [21] N. N. Achasov and E. V. Rogozina, Mod. Phys. Lett. A, 30 (2015) 1550181, arXiv:1501.03583.
- [22] C. Hanhart, Y. S. Kalashnikova, and A. V. Nefediev, Eur. Phys. J. A47 (2011) 101, arXiv:1106.1185.